

**2016 NDIA GROUND VEHICLE SYSTEMS ENGINEERING AND TECHNOLOGY SYMPOSIUM
AUTONOMOUS GROUND SYSTEMS (AGS) TECHNICAL SESSION
AUGUST 2-4, 2016 - NOVI, MICHIGAN**

**SIMULATION-BASED PROTOTYPING OF STABILITY CONTROL CONCEPTS
FOR HIGH-SPEED TELEOPERATION OF HEAVY VEHICLES**

Jia-Hsuan Lo, PhD

Sean Eye

Steve M. Rohde, PhD

Mitchell M. Rohde, PhD

Quantum Signal, LLC

200 N. Ann Arbor St., Saline, MI 48176

www.quantumsignal.com

ABSTRACT

Teleoperated ground vehicles are an integral part of the U.S. Army and Marine Corps long range vision and a key transition technology for fully autonomous vehicles. However, the combination of marginally-stable vehicle dynamics and limited perception are a key challenge facing teleoperation of such platforms at higher speeds. New technologies for enhancing operator perception and automatically detecting and mitigating rollover risk are needed to realize sufficient safety and performance in these applications. This paper presents three rollover mitigation concepts for high speed teleoperation of heavy tactical vehicles, including model-predictive warning, negative obstacle avoidance, and reactive brake controls. A modeling and simulation approach was used to evaluate these concepts within the Autonomous Navigation Virtual Environment Laboratory (ANVEL). Vehicle models for both the M1078 cargo truck and RG-31 MRAP were used throughout concept evaluation over terrain ranging from urban highway to off-road conditions with more complex topography.

Introduction

Teleoperated unmanned ground vehicles significantly reduce both personnel exposure to hazardous situations and required, human-centric logistics support. However, because the teleoperator's situational awareness about the vehicle and environment are monitored by electronic sensors and relayed through the communications link to the control unit, important human-based sensing such as stereo vision and vestibular perception are usually not available. Further, heavier tactical vehicles have high centers of gravity and unique handling characteristics which lead to a significant number of rollover incidents, even when manually-driven. While many advances have been made in the commercial passenger vehicle domain to improve vehicle safety—including technology such as adaptive cruise control, and roll/yaw stability control—such technology, surprisingly, has not been introduced to military vehicles.

Not all rollovers are caused by the same mechanism. A US Marine Corps safety document (Dunard, 2008) indicated that the majority of rollover incidents for mine-resistant, ambush-protected (MRAP) vehicles are initiated by following mechanisms: (1) fall initiated: occurred due to ledge, slope or

ground surface collapse; (2) maneuver initiated: swerving maneuver on flat ground or terrain; and (3) impact initiated: object collision caused rollover. From the same report (Dunard, 2008), a snapshot of the rollover trend from October 2007 to October 2008 shows that 41% of the rollovers were fall-initiated, 31% of them are maneuver-initiated, and 4% were impact-initiated. Therefore, the ability to predict fall- and maneuver-initiated rollovers covers the most rollover situations and provides the greatest benefit.

To prevent fall- and maneuver-initiated rollover incidents for high speed teleoperation of heavy tactical vehicles, the stability enhancement technology should contain both a predictive capability (where the system monitors the upcoming terrain and obstacle conditions and operator inputs, and predicts vehicle stability) and a reactive capability (where the vehicle's stability is monitored and maintained continuously). The system should also be low cost, and adaptable to a wide range of legacy vehicles of varying size and type.

Here we present three rollover mitigation concepts, including steering constraint control, negative obstacle avoidance control, and reactive brake control. The first concept is designed for mitigating maneuver-initiated rollovers; the

second concept (negative obstacle avoidance) for preventing fall-initiated rollovers; and the last one (reactive brake) for reducing the rollover risks to both maneuver- and fall-initiated cases. These concepts were developed, prototyped, and characterized using modeling and simulation (M&S) within the Autonomous Navigation Virtual Environment Laboratory (ANVEL). An M&S approach was adopted to reduce development time, expand the variety of scenarios and maneuvers which could be analyzed, and allow for systematic exploration of designs. Vehicle models for the RG-31 MRAP were used throughout concept evaluation over terrain ranging from urban highway to off-road conditions with more complex topography. In addition, a Kawasaki Mule model and actual vehicle were used for initial studies and to validate the M&S approach.

In the next section ANVEL and its capabilities are briefly discussed, including some recent validation studies. In the following section the no-rollover steering constraint control method is described, and the results of simulation studies are presented. Next, negative obstacle detection and avoidance control is presented followed by a description of a reactive rollover brake control module that aims to maintain vehicle stability while adhering to the operator's intent. That module monitors vehicle acceleration and rotational kinematics and then performs feedback brake control to stabilize the vehicle when necessary. In the final sections of this paper the efficacy of the three approaches are discussed and future research efforts suggested.

ANVEL

ANVEL was specifically designed to bootstrap the development of unmanned ground systems and facilitates creation, development, verification, validation, and deployment of semi-autonomous and autonomous behavior software. It delivers a unique combination of vehicle, sensor, and vehicle-terrain interaction (VTI) models; a robust physics engine; and a terrain editor that enables the creation of systems and scenarios for development of semi-autonomous and autonomous behaviors. Platforms are modeled using a vehicle definition file. Creating new platforms or modifying existing platforms (Figure 1) is as simple as changing the file. Users can easily alter vehicle mass, drag coefficient, surface area, wheel base, track width, tire size and stiffness, sensor types/positions and more. In this paper we modeled a Kawasaki Mule used to experimentally evaluate some of the perception and control concepts, the M1078 cargo truck, and the RG-31 MRAP. The models can also include major vehicle subsystems such as engines, transmissions, and electric motors. ANVEL provides a high degree of flexibility when creating a system model to enable the appropriate fidelity for the task at hand.



Figure 1: Examples of platforms modeled in ANVEL.

ANVEL also includes a number of exteroceptive and proprioceptive sensor models. Notably, ANVEL models a single line scan LIDAR sensor that can be parametrically adjusted to characteristics of commonly available commercial LIDAR systems, such as the SICK LMS-5xx and the Hokuyo UTM-30LX. Multi-beam LIDARs such as the Velodyne HDL64 are also modeled. Proprioceptive sensing includes various inertial measurement unit components, including micro-electrical mechanical accelerometers and gyroscopes. New sensor models can be readily developed and implemented through the use of a plug-in architecture, allowing for the simulation of nearly any kind of sensor, including geometric, inertial, force-torque, or global positioning.

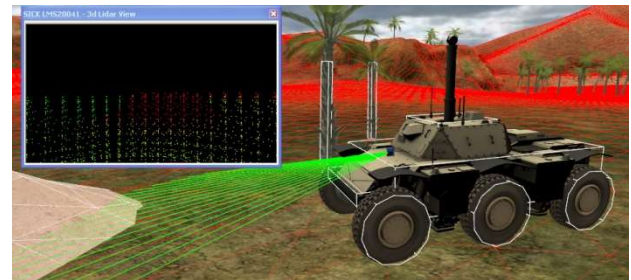


Figure 2: Example of a SICK LIDAR modeled in ANVEL.

Enabling the vehicle models and sensors to interact with the “world” is the core of the simulation tool and ANVEL currently uses the Open Dynamics Engine (ODE) to enable real-time simulation of the vehicle bodies in the virtual environment. ODE simulates articulated rigid body structures and the forces that act on those structures. The bodies consist of mass, position, shape, and orientation and they are articulated by joints that specify the type of motion between the bodies. Joint types include specific instances of prismatic, revolute, and spherical assemblies. The bodies can also have constraints placed upon them, such as the range of motion or force limits. In ANVEL, the physics of vehicles are modeled as a combination of shapes, and terrain is modeled using a polygon mesh. Rendering of the vehicles and terrain can use higher resolution mesh representations appropriate for graphical display.

By representing the terrain as a polygonal mesh, ANVEL is able to use various VTI models that simulate the forces between the wheel contact patch and the virtual terrain. These include an ODE VTI model and a Pacejka model. The ODE VTI model is like all other body interactions within ODE: hard contacts with a non-penetration constraint. The Pacejka VTI plugin models a pneumatic tire against the terrain. These VTI models allow the operator to utilize the appropriate ground or tire model in the simulation, enabling the proper fidelity ground-tire model for the required task. Additional VTI models can be created and applied to ANVEL through its plug-in infrastructure.

ANVEL ties the ODE physics engine, VTI models, vehicle models, and sensors together through the use of a world editor. The editor permits users to specify the ground contours, vegetation, man-made structures, and robot positions and orientations, allowing for the creation of a number of virtual environments and scenarios for experimentation. Indoor and outdoor environments can be created and manipulated. This capability allows for virtual testing that enables rapid identification and resolution of scenarios that may prove error-prone or require a repeatable test environment for debugging, data collection, and subsequent analysis. These virtual worlds can also be used to revalidate behaviors and potential concepts of operation (CONOPS) as systems evolve throughout the course of the normal development cycle.

ANVEL Model Validation

For validation of the ANVEL models, two vehicle models were constructed. The first was a detailed sport utility vehicle model to compare with the generic D-Class SUV template model in CarSim, a widely used multibody dynamics simulation program. The ANVEL model parameters were derived from the CarSim D-Class model. The second validation model was for a Kawasaki 4010 Mule UTV used as a testbed vehicle by Quantum Signal, LLC. Defining the Mule model in CarSim required measurement and estimation of several additional vehicle parameters and lead to a detailed model of the Mule.

Maneuvers conducted on each of the two vehicle models included a double lane change maneuver at 50 km/hr. The kinematics and tire loading data were collected and compared.

A three-phase validation procedure comparing experimental data to simulation data from both CarSim and ANVEL was pursued where possible. While comparison to experimental data is the “gold standard,” the use of high-fidelity simulation data provides significant flexibility (such as testing scenarios that would be difficult or dangerous to test experimentally, or in studying the effect of parameter variation on model outputs).

As shown in Figure 3 and Figure 4, good agreement was found in the road wheel steer angle and slip angle between ANVEL and CarSim. Because both models were given the same steering wheel angle input, this result indicates both models have similar steering actuation dynamics and cornering stiffness.



Figure 3: Wheel steer angle for both ANVEL and CarSim models in the double lane change test.

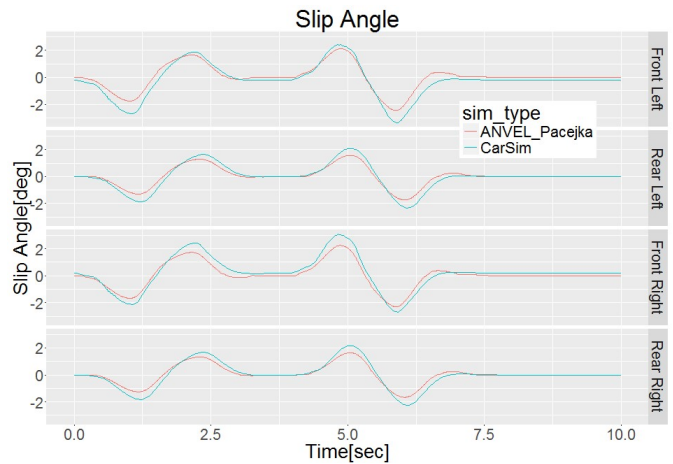


Figure 4: Slip angle for both ANVEL and CarSim models in the double lane change test.

Figure 5 and Figure 6 show the angular kinematics and tire normal force of both ANVEL and CarSim vehicle models. In general, good agreement is observed. Although some discrepancy is found in the magnitude of the roll angle and rear tire normal forces, the overall trend between ANVEL and CarSim results agree well.

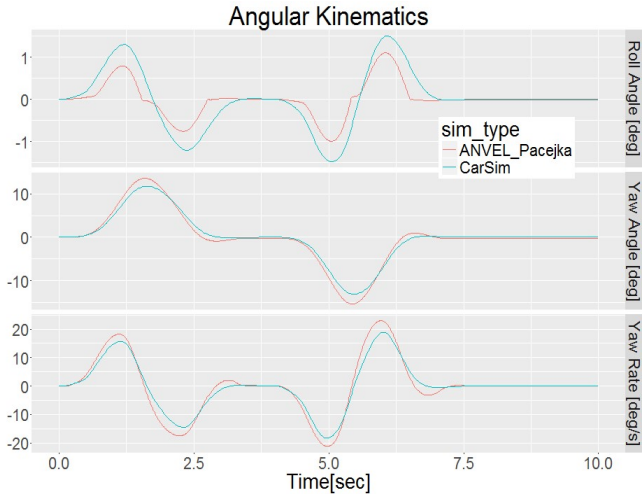


Figure 5: Front axle steering angle constant radius turn with large steering angle.

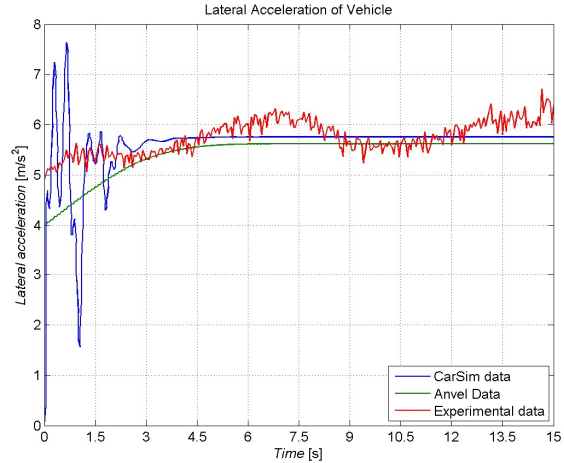


Figure 7: Lateral acceleration of vehicle for constant radius turn with moderate steering angle.

For most of the kinematic and kinetic variables, the ANVEL model results agreed well with the CarSim model, and with the limited experimental data that was collected. We believe, at least for the conceptual design purposes, the fidelity that ANVEL provides is more the adequate, and our rollover stability control concepts were all developed and optimized within ANVEL environment.

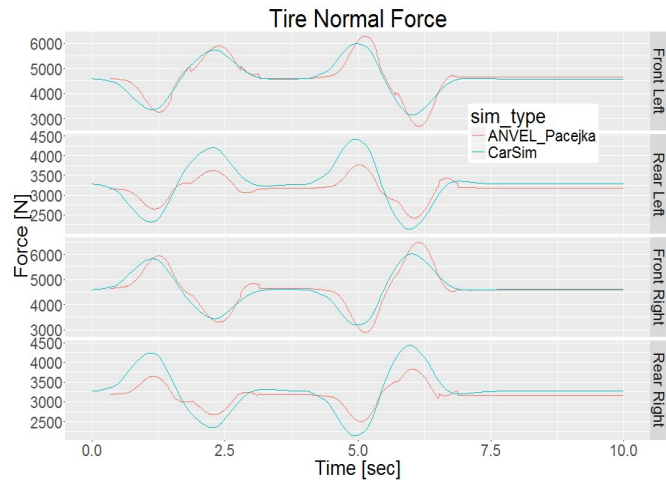


Figure 6: Tire normal force during the double lane change maneuver.

Agreement of simulation results with experimental data was also quite good. Figure 7 shows experimental data from the Kawasaki Mule, for constant radius turn with a moderate steering angle maneuver. Good agreement between CarSim, ANVEL, and the Mule data can be observed, with the most significant discrepancy present in lateral acceleration, which again was likely caused by 1) sensor noise and 2) natural terrain variation inherent in experimental testing.

Steering Constraint Control to Prevent Maneuver-Initiated Rollovers

For a maneuver-initiated rollover in teleoperation settings, it has been shown that the common cause is that the operator over-steers the vehicle due to inexperience, communication delay, and/or inefficient visual and kinesthetic feedback (McGovern, 1989). To prevent maneuver-initiated rollovers, maintaining the steering input within a safe region is essential. Therefore, we propose a constraint-based steering control algorithm. The on-board computer considers the current vehicle status – such as speed, steering, and rotational kinematics – and computes a recommended allowable steering range. This no-rollover steering range provides the information about the vehicle’s current limitation to perform a safe maneuver. Beyond that range, vehicle stability is no longer guaranteed.

This steering constraint estimation can be presented to the operator as a simple numeric indicator or a highlighted no-rollover steering range graphic to inform the operator whether the current steering maneuver is potentially hazardous (Figure 8). This estimation was also implemented as the steering

lower- and upper-bounds to prevent the driver from driving too aggressively.

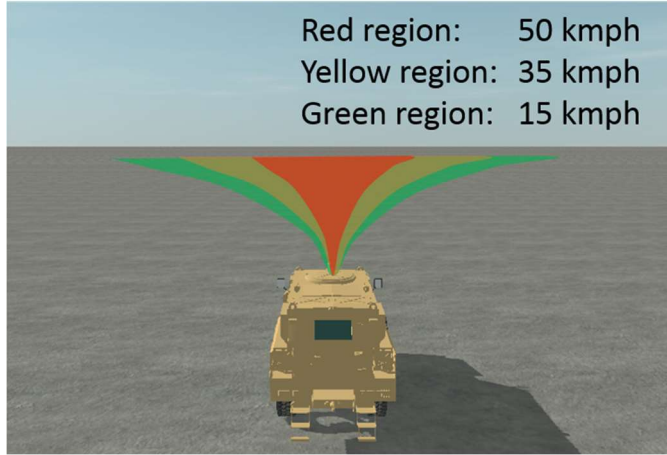


Figure 8: Illustration of a conceptual no-rollover steering range display. The no-rollover steering range is adaptively adjusted depending on the current vehicle speed.

To estimate the no-rollover steering range, a state-space vehicle model was constructed as the predictive model. The detailed model derivation was based on the published model (Zak, 2007). The tire normal force in the model can be expressed in the following form:

$$f_{tire} = f(\phi, a_x, a_y) \quad (1)$$

where ϕ is the vehicle roll angle, and a_x and a_y are the longitudinal and lateral accelerations. The model takes the roll angle signal from the ANVEL vehicle simulation as the input. By assuming the vehicle is moving forward at a constant speed ($a_x = 0$), the value of lateral acceleration a_y can be determined. Then, by applying the following approximated kinematics and geometric calculations, the maximal steering angle can be estimated:

$$a_y = \frac{v_x^2}{R} = \frac{v_x^2 \tan(\delta_{max})}{L} \Rightarrow \delta_{max} = \tan^{-1}\left(\frac{La_y}{v_x^2}\right) \quad (2)$$

The symbol R represents the current vehicle turning radius; L is the wheel base; and δ_{max} is estimated no-rollover steering range.

To verify the accuracy of this no-rollover steering estimation, a rollover simulation was conducted using RG-31 MRAP as the test vehicle. In the simulation, the vehicle was accelerated from stationary to a prescribed constant speed. Once the

specified speed was reached, the steering was gradually increased until the rollover occurred. The estimated no-rollover steering range was continuously computed, and the actual rollover steering angle was recorded. Various speeds, from 10 to 20 m/s, were tested and the estimated and actual rollover steering angles were compared.

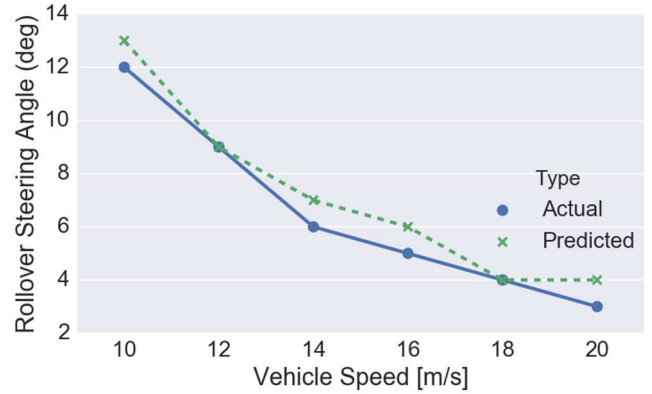


Figure 9: Comparison between predicted and actual steering angle at rollover.

As seen in Figure 9, the results show that the predicted and actual rollover steering angles differs by one degree or less. It should be noted that this method provides accurate estimates under the assumption that the information about the current vehicle payload is known. Without the payload information, the rollover steering estimation may be erroneous, and a conservative approach should be adopted (i.e., using greater payload to estimate the rollover steering range).

Negative Obstacle Avoidance Control to Prevent Fall-Initiated Rollovers

Military ground vehicle transportation applications must accommodate off-road terrain, and, therefore, accurately assessing the traversability of the off-road terrain is important. Detecting negative obstacles, such as large pot-holes, ditches, and road-side slopes, plays a vital role in avoiding fall-initiated rollovers. However, in general negative obstacles are difficult to detect, especially at long ranges. Various video- (A. Rankin, 2005; Witus, Karlsen, Gorsich, & Gerhart, 2001); thermal- (Rankin, 2003); and lidar-based (Larson & Trivedi, 2011; Heckman, Lalonde, N., & Hebert, 2007; Heckman, Lalonde, N., & Hebert, 2007) detection methods have been proposed in the literature to tackle this problem. Each method has its own advantages and limitations, as the negative obstacle detection is still an on-going research problem.

In this paper, the main focus is to demonstrate the benefit of negative obstacle detection in preventing fall-initiated rollovers. Therefore, a simple version of negative obstacle detection scheme was implemented based on the method reported in Larson & Trivedi. It uses occlusions of lidar points to identify potential negative obstacles in the distance and then examines the terrain down- and up-hill slopes to confirm the negative obstacle detection as the vehicle gets closer. The algorithm is illustrated in Figure 10.

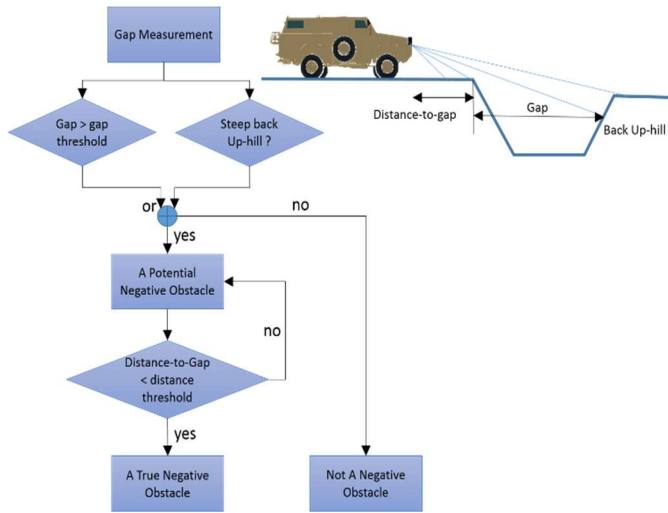


Figure 10: Negative obstacle detection flow-chart.

Along with the negative obstacle detection algorithm, an adaptive speed control was also implemented on the ANVEL-simulated RG-31 to ensure the vehicle stops completely in front of a negative obstacle. The principle is to adjust the throttle to maintain a safe distance to the negative obstacle in front. When the distance is reduced near the minimal allowable braking distance of the vehicle, an emergency brake control is activated to fully stop the teleoperated vehicle.

Reactive Rollover Brake Control to Maintain Vehicle Stability

An Army study of 464 rollover mishaps during the period January 2003 through April 2006 reported that the most common sources of MRAP rollovers is the excessive speed (Dunard, 2008). This same study also noted that driver-based mistakes accounted for 52% of the rollovers. These facts indicate that reducing the vehicle speed while initiating a steering maneuver or traversing uneven terrain is a must. However, human driver often misjudge the vehicle’s speed and/or maneuver capability.

To prevent rollovers due to driver mistakes, a reactive rollover brake control was implemented in the ANVEL RG-31 vehicle

based on a roll stability control system used on passenger vehicles (Lu, Messih, & Salib, 2007). The algorithm inhibits vehicle roll tendency through reactive braking based on four proportional feedback controls (front slip, yaw rate, roll angle, and roll rate) and is illustrated in Figure 11.

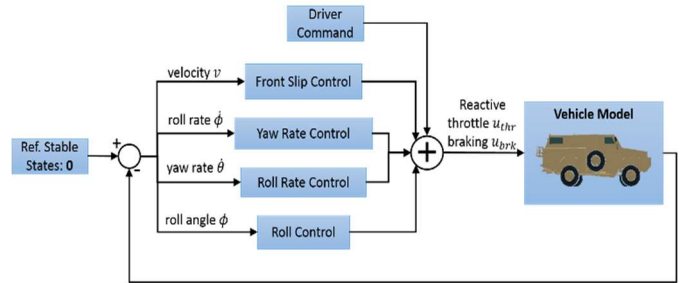


Figure 11: Reactive brake control diagram.

It is worth noting that while the vehicle is moving on flat terrain at a slow speed (such as 4 m/s) and assuming no impact occurs, the vehicle simply does not have sufficient momentum to roll over even under an aggressive steering maneuver. For that reason, it is necessary to fine tune the controller gain according to the current vehicle speed. In our design, the proportional controller gains are expressed as sigmoid functions. As an example, the roll feedback gain is in the following format:

$$k_{roll} = 0.02 + \frac{1}{1 + \exp(-2.5 * (vx - 6))}$$

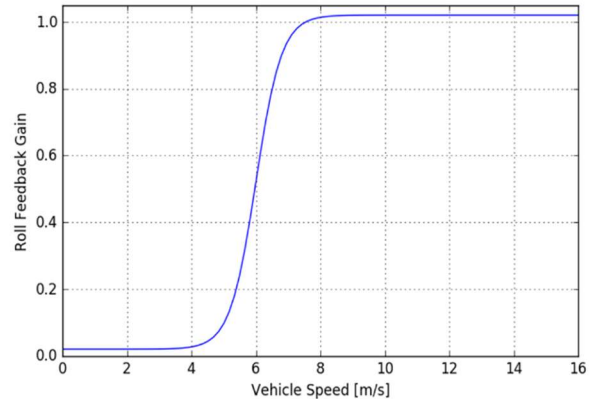


Figure 12: Sample roll angle feedback control gain.

As shown in Figure 12, the roll angle feedback gain maintains a minimum level of 0.02 while the vehicle speed is slow (less than 5 m/s) and rapidly increases to 1.02 when the vehicle speed approaches to 8 m/s. This arrangement ensures that the reactive brake does not activate at a low vehicle speed when it is not needed, but intervenes at a greater speed when necessary.

Evaluation of the Rollover Stability Control Concepts

To explore whether the aforementioned rollover control concepts can effectively prevent vehicle rollovers, automated path-following simulation tests were conducted. The “test vehicle” was an ANVEL RG-31 model. Two planar lidar sensors were mounted on the vehicle, one at the driver’s side corner, and the other at passenger’s side corner. The orientations of the lidar sensors were setup to scan vertically, so the ground profile could be captured in detail. The lidar sensors were also rotated outwards by 10 degrees to allow a wider detection range (Figure 13).

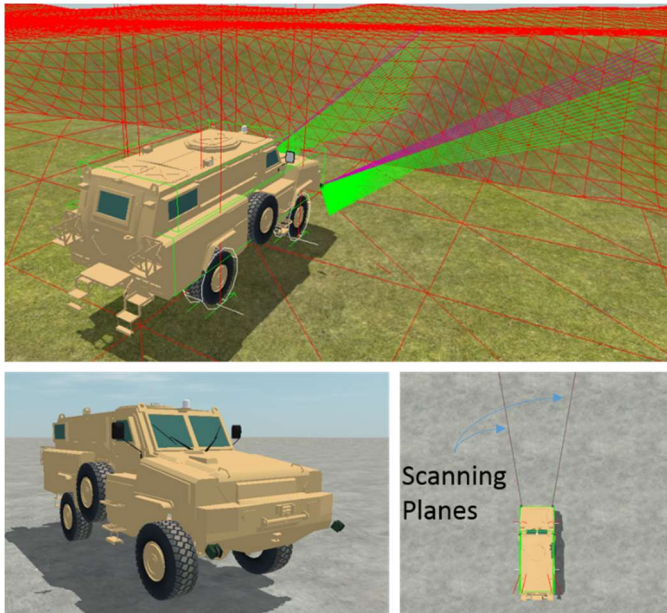


Figure 13: ANVEL RG-31 vehicle lidar sensors arrangement.

The no-rollover steering constraint, negative obstacle avoidance and reactive brake controls were integrated in the RG-31 vehicle model. Because each module addresses independent issues leading to rollovers, their functions are complimentary to one another, and, thus, the integration is straightforward. For convenience, this rollover control system is called Rollover Guarded Motion Controls (RGM).

For the fall-initiated rollover scenario, we performed simulation runs on two different obstacle types: (1) a large pothole, and (2) a road-side slope. The test vehicle model (RG-31) followed several predefined routes leading to the obstacles. For each route, two simulation runs were performed, one with and the other without the RGM system, and the rollover outcome was observed.

For testing the maneuver-initiated rollovers, the vehicle followed a predefined route on a flat concrete surface and an uneven terrain with various forward speeds (Figure 14). The route was designed to include sharp turns to induce vehicle rollover behavior. Again, the vehicle was tested on each route with and without the RGM. The time required to finish the route and the vehicle rollover outcome were observed.

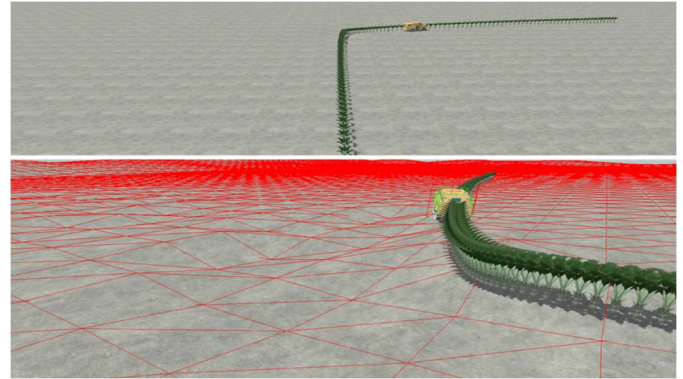


Figure 14: Predefined route in the maneuver-initiated rollover test, marked by palm trees for illustration purposes. The top figure shows the sharp turn designed to induce a rollover; and the bottom figure shows the uneven terrain that presents a greater risk to rollover.

Fall-Initiated Rollover Simulation Results

Pothole Test

A large pothole is located on a grass field. The test vehicle approached the pothole from eight different angles (Figure 15). In the test, the baseline vehicle without RGM fell into the pothole from all approaching angles, while the test vehicle with RGM successfully detected and stopped in front of the pothole in seven out of eight routes (Figure 16).

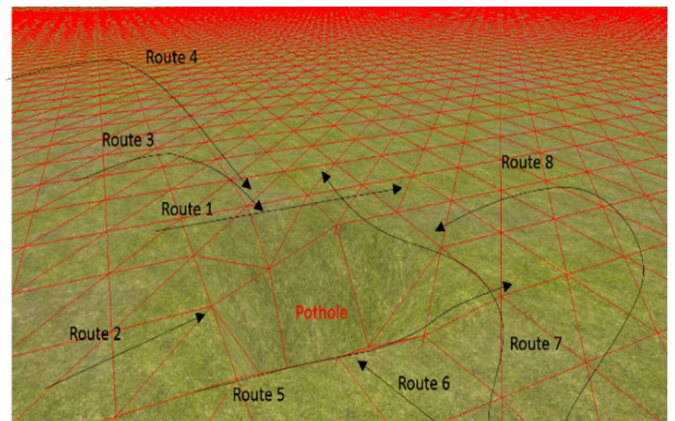


Figure 15: Pothole test routes.



Figure 16: Sample simulation screenshots showing that the test vehicle with RGM successfully stopped in front of a pothole, while the baseline vehicle fell in.

Route three is the only approaching angle where the RGM vehicle failed to avoid the pothole because the route abruptly turned into the direction heading to the pothole. The test vehicle RG-31 detected the hole but simply did not have enough time and distance to fully stop itself.

Road-side Slope Test

The test vehicle drove around a canyon-type terrain. Several driving routes were designed so that one side of the wheels approached road-side slopes (Figure 17). The baseline test vehicle inevitably fell into the canyon from road-side slopes, while the vehicle equipped with RGM successfully avoided falling in five out of five routes (Figure 18).

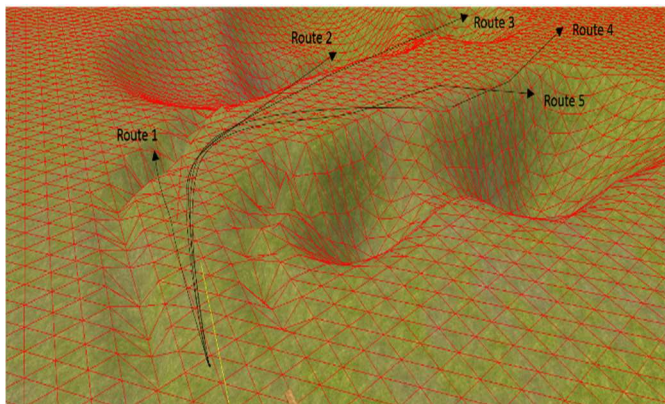


Figure 17: Routes in road-side slope test.



Figure 18: Sample simulation screenshots showing that the test vehicle with RGM successfully stopped in front of a road-side slope, while the baseline vehicle fell down the slope.

Maneuver-initiated Rollover Simulation Results

On Flat Surface

As observed in Figure 20, the baseline test vehicle was able to complete the design route on flat terrain shown previously in Figure 14 without rolling over at a speed up to 9 m/s. The vehicle with RGM was capable of inhibiting rollover at forward speeds up to 15 m/s.

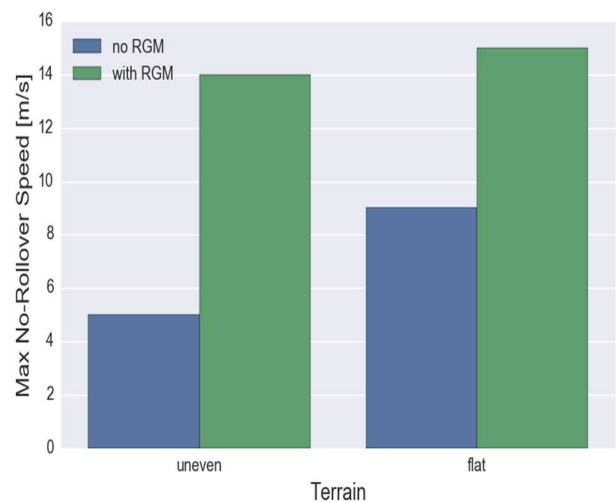


Figure 19: Maximal vehicle speeds without rollover in the maneuver test.

On Uneven Terrain

Uneven terrain presents a challenge to the steering maneuver due to its unpredictability. In this test, both the baseline and RGM-equipped vehicle must reduce speed to avoid rollover. The maximum no-rollover forward speed for the baseline vehicle and the vehicle with RGM were 5 m/s and 14 m/s, respectively.



Figure 20: Sample screenshots showing the difference between the baseline vehicle and the one with RGM. Solid images represent the vehicle with RGM; opaque images are the baseline vehicle. The forward speed was 8 m/s for both vehicles in this test.

Discussion

This simulation study demonstrates the potential of rollover stability control, including no-rollover steering constraint, negative obstacle avoidance, and reactive brake control, in reducing rollover incidences. With a high weight as well as center of mass, military tactical vehicles are inherently difficult to operate. Rollover prediction and intervention systems such as the RGM proposed in this paper are warranted, and our results show that a rollover incident may be prevented in many situations by introducing some type of stability control system in the vehicle.

The ANVEL simulation approach used in this study allows for quick feasibility checks on the conceptual design without implementing expensive and time-consuming hardware experiments. Moreover, broader design spaces that cannot be investigated in hardware experiments due to safety reasons can be explored. For example, in this simulation study, we are able to force the vehicle to roll over using aggressive maneuvers to understand the limits of the control capabilities: it is difficult, costly, and dangerous to do this using an experimental approach.

There are several limitations in the present study. First, the RG-31 MRAP vehicle model is not fully validated. The vehicle dynamics parameters were tuned to meet the specifications obtained from TARDEC internal data, as well as the manufacturer. However, since instrumented vehicle dynamic test results for RG-31 were not available, except for linear acceleration performance and gradability, the fidelity of other dynamics aspects in this ANVEL RG-31 model is unknown. Second, the sensor error model is simplified as Gaussian distributions, which may not accurately represent realistic performance. Lastly, the path following behavior is simplified in the test: no driver model was implemented in the route following task.

With the limitations mentioned above, quantitative interpretation of the study results should be cautious. However, as pointed out earlier, this study mainly focused on the conceptual design and feasibility check of the rollover control. It clearly qualitatively demonstrates the potential and benefits of a stability control system, such as the RGM system proposed in our study to reduce the risk of rollover.

The rollover guarded-motion system was designed by tackling individual mechanisms (i.e. fall- and maneuver-initiated) of rollovers. This strategy helps simplify the control system design, as each module has clearly defined functionality, tackles a specific problem, and minimizes the overlaps and/or conflicts among modules. With the ANVEL simulation tool, the vehicle model, terrain, sensor parameters, and environment setups can be easily tailored to specific settings, which facilitates our trade study and optimization of the controllers.

Conclusions

The proposed rollover guarded motion control concepts, including negative obstacle avoidance, no-rollover steering range constraint, and reactive brake control, show potentials in reducing fall- and maneuver-initiated rollovers. The authors advocate the use of a simulation paradigm for conceptual design of vehicle control systems, as it provides benefits of lower cost, reduced design time, minimal safety concern, and versatility for mobile robotics system design.

The authors gratefully acknowledge the support of the US Army for this work via contracts W56HZV-15-C-0169 and W56HZV-14-C-0052.

References

- A. Rankin, A. H. (2005). Evaluation of stereo vision obstacle detection algorithms for off-road autonomous navigation. *AUVSI Symposium on Unmanned Systems*.
- Dunard, M. (2008). *The Safety Corner - This Issue of the Safety Corner Highlights Best Practices for Preventing/Mitigating Vehicle Rollovers*. Marine Corps Center for Lessons Learned (MCCLL).
- Heckman, N., Lalonde, J., N., V., & Hebert, M. (2007). Potential negative obstacle detection by occlusion labeling. *Proceedings of International Conference on Intelligent robots and Systems (IROS)*.
- Larson, J., & Trivedi, M. (2011). Lidar Based Off-road Negative Obstacle Detection and Analysis. *14th International IEEE Conference on Intelligent Transportation Systems*, (pp. 192-197). Washington, DC, USA.
- Lu, J., Messih, D., & Salib, A. (2007). Roll rate based stability control - the Roll Stability Control (TM) System. *Proceedings of 20th International Technical Conference on the Enhanced Safety of Vehicles*. 07-136, pp. Ford RSC 1-13. Lyon, France: NHTSA.
- McGee, H. W., Hooper, K. G, Hughes, W. E, & Benson W. (1983). *Highway Design and Operation Standards Affected by Driver Characteristics: Volume II: No FHWA-RD-83-015*. Vienna, Virginia, USA: Bellomo-McGee Inc.
- McGovern, D. E. (1989). Experiences in teleoperation of land vehicles. *MAN/SYSTEM TECHNOLOGY AND LIFE SUPPORT* (pp. 38-1 - 38-11). Albuquerque, NM, United States: NASA, Ames Research Center, Spatial Displays and Spatial Instruments;
- Rankin, L. M. (2003). Negative obstacle detection by thermal signature. *Proceedings of 2003 IEEE/RSJ International Conference on Intelligent Robots and Systems (IROS)*, (pp. 906-913).
- Rohde, M. M. (2014). *Approach to CG Height Estimation & Description of the ANVEL-Based Predictive Stability Engine*. Warren, MI: U.S. Army TARDEC.
- Witus, G., Karlsen, R. E., Gorsich, D. J., & Gerhart, G. R. (2001). Preliminary investigation into the use of stereo illumination to enhance mobile robot terrain perception. *Proceedings of the SPIE 4364: Unmanned Ground Vehicle Technology III*, 290, (pp. 290-301).
- Zak, A. B. (2007). Modeling the Control of an Automated Vehicle, Vehicle System Dynamics. *International Journal of Vehicle Mechanics and Mobility*(Jul), 131-155.